Clin Orthop Relat Res (2020) 00:1-14
DOI 10.1097/CORR.0000000000001449

Clinical Orthopaedics and Related Research®
A Publication of The Association of Bone and Joint Surgeons®

Basic Research

Radiation Disrupts the Protective Function of the Spinal Meninges in a Mouse Model of Tumor-induced Spinal Cord Compression

Takaki Shimizu MD, Satoru Demura MD, PhD, Satoshi Kato MD, PhD, Kazuya Shinmura MD, PhD, Noriaki Yokogawa MD, PhD, Noritaka Yonezawa MD, Norihiro Oku MD, Ryo Kitagawa MD, Makoto Handa MD, Ryohei Annen MD, Takayuki Nojima MD, PhD, Hideki Murakami MD, PhD, Hiroyuki Tsuchiya MD, PhD

Received: 5 March 2020 / revised: 1 July 2020 / Accepted: 16 July 2020 / Published online: 17 August 2020

Abstract

Background Recent advances in multidisciplinary treatments for various cancers have extended the survival period of patients with spinal metastases. Radiotherapy has been widely used to treat spinal metastases; nevertheless, long-term survivors sometimes undergo more surgical intervention after radiotherapy because of local tumor relapse. Generally, intradural invasion of a spinal tumor seldom occurs because the dura mater serves as a tissue barrier against tumor infiltration. However, after radiation exposure, some spinal tumors invade the dura mater, resulting in leptomeningeal dissemination, intraoperative dural injury, or postoperative local recurrence. The mechanisms of how radiation might affect the dura have not been well-studied.

Questions/purposes To investigate how radiation affects the spinal meninges, we asked: (1) What is the effect of irradiation on the meningeal barrier's ability to protect against carcinoma infiltration? (2) What is the effect of irradiation on the meningeal barrier's ability to protect against sarcoma infiltration? (3) What is the effect of irradiation on dural microstructure observed by scanning electron microscopy (SEM)? (4) What is the effect of irradiation on dural microstructure observed by transmission electron microscopy (TEM)?

Methods Eighty-four 10-week-old female ddY mice were randomly divided into eight groups: mouse mammary tumor (MMT) implantation 6 weeks after 0-Gy irradiation (nonirradiation) (n = 11), MMT implantation 6 weeks after 20-Gy irradiation (n = 10), MMT implantation 12 weeks after nonirradiation (n = 10), MMT implantation 12 weeks after 20-Gy irradiation (n = 11), mouse osteosarcoma (LM8) implantation 6 weeks after nonirradiation (n = 11), LM8 implantation 6 weeks after 20-Gy irradiation (n = 11), LM8 implantation 12 weeks after nonirradiation (n = 10), and LM8 implantation 12 weeks after 20-Gy irradiation (n = 10); female mice were used for a mammary tumor

The institution of one or more of the authors (HM, TS) have received, during the study period, funding from the Japan Society for the Promotion of Science KAKENHI Grant No. 17K10927 and the Radiation Effects Association.
Each author certifies that neither he, nor any member of his immediate family, has any commercial associations (consultancies, stock ownership, equity interest, patent/licensing arrangements, etc.) that might pose a conflict of interest in connection with the submitted article.
Each author certifies that his institution approved the animal protocol for this investigation and that all investigations were conducted in conformity with ethical principles of research.
This work was performed at Kanazawa University, Kanazawa, Japan.

T. Shimizu, S. Demura, S. Kato, K. Shinmura, N. Yokogawa, N. Yonezawa, N. Oku, R. Kitagawa, M. Handa, R. Annen, T. Nojima, H. Tsuchiya, Department of Orthopaedic Surgery, Graduate School of Medical Sciences, Kanazawa University, Kanazawa, Japan

H. Murakami, Department of Orthopaedic Surgery, Nagoya City University Graduate School of Medical Sciences, Nagoya, Japan

S. Demura (✉), 13-1 Takara-machi, Kanazawa 920-8641, Japan, Email: demudon@med.kanazawa-u.ac.jp

All ICMJE Conflict of Interest Forms for authors and *Clinical Orthopaedics and Related Research*® editors and board members are on file with the publication and can be viewed on request.

Wolters Kluwer

metastasis model and ddY mice, a closed-colony mice with genetic diversity, were selected to represent interhuman diversity. Mice in each group underwent surgery to generate a tumor-induced spinal cord compression model at either 6 weeks or 12 weeks after irradiation to assess changes in the meningeal barrier's ability to protect against tumor infiltration. During surgery, the mice were implanted with MMT (representative of a carcinoma) or LM8 tumor. When the mice became paraplegic because of spinal cord compression by the growing implanted tumor, they were euthanized and evaluated histologically. Four mice died from anesthesia and 10 mice per group were euthanized (MMT-implanted groups: MMT implantation occurred 6 weeks after nonirradiation [n = 10], 6 weeks after irradiation [n = 10], 12 weeks after nonirradiation [n = 10], and 12 weeks after irradiation [n = 10]; LM8-implanted groups: LM8 implantation performed 6 weeks after non-irradiation [n = 10], 6 weeks after irradiation [n = 10], 12 weeks after nonirradiation [n = 10], and 12 weeks after irradiation [n = 10]); 80 mice were evaluated. The spines of the euthanized mice were harvested; hematoxylin and eosin staining and Masson's trichrome staining slides were prepared for histologic assessment of each specimen. In the histologic assessment, intradural invasion of the implanted tumor was graded in each group by three observers blinded to the type of tumor, presence of irradiation, and the timing of the surgery. Grade 0 was defined as no intradural invasion with intact dura mater, Grade 1 was defined as intradural invasion with linear dural continuity, and Grade 2 was defined as intradural invasion with disruption of the dural continuity. Additionally, we euthanized 12 mice for a microstructural analysis of dura mater changes by two observers blinded to the presence of irradiation. Six mice (three mice in the 12 weeks after non-irradiation group and three mice in the 12 weeks after 20-Gy irradiation group) were quantitatively analyzed for defects on the dural surface with SEM. The other six mice (three mice in the 12 weeks after nonirradiation group and three mice in the 12 weeks after 20-Gy irradiation group) were analyzed for layer structure of collagen fibers constituting dura mater by TEM. In the SEM assessment, the number and size of defects on the dural surface on images (200 μm × 300 μm) at low magnification (× 2680) were evaluated. A total of 12 images (two per mouse) were evaluated for this assessment. The days from surgery to paraplegia were compared between each of the tumor groups using the Kruskal-Wallis test. The scores of intradural tumor invasion grades and the number of defects on dural surface per SEM image were compared between irradiation group and non-irradiation group using the Mann-Whitney U test. Interobserver reliabilities of assessing intradural tumor invasion grades and the number of dural defects on the dural surface were analyzed using Fleiss'κ coefficient. P values < 0.05 were considered statistically significant.

Results There was no difference in the median (range) time to paraplegia among the MMT implantation 6 weeks after nonirradiation group, the 6 weeks after irradiation group, the 12 weeks after nonirradiation group, and the 12 weeks after irradiation group (16 days [14 to 17] versus 14 days [12 to 18] versus 16 days [14 to 17] versus 14 days [12 to 15]; χ^2 = 4.7; p = 0.19). There was also no difference in the intradural invasion score between the MMT implantation 6 weeks after irradiation group and the 6 weeks after non-irradiation group (8 of 10 Grade 0 and 2 of 10 Grade 1 versus 10 of 10 Grade 0; p = 0.17). On the other hand, there was a higher intradural invasion score in the MMT implantation 12 weeks after irradiation group than the 12 weeks after non-irradiation group (5 of 10 Grade 0, 3 of 10 Grade 1 and 2 of 10 Grade 2 versus 10 of 10 Grade 0; p = 0.02). Interobserver reliability of assessing intradural tumor invasion grades in the MMT-implanted group was 0.94. There was no difference in the median (range) time to paraplegia among in the LM8 implantation 6 weeks after nonirradiation group, the 6 weeks after irradiation group, the 12 weeks after non-irradiation group, and the 12 weeks after irradiation group (12 days [9 to 13] versus 10 days [8 to 13] versus 11 days [8 to 13] versus 9 days [6 to 12]; χ^2 = 2.4; p = 0.50). There was also no difference in the intradural invasion score between the LM8 implantation 6 weeks after irradiation group and the 6 weeks after nonirradiation group (7 of 10 Grade 0, 1 of 10 Grade 1 and 2 of 10 Grade 2 versus 8 of 10 Grade 0 and 2 of 10 Grade 1; p = 0.51), whereas there was a higher intradural invasion score in the LM8 implantation 12 weeks after irradiation group than the 12 weeks after nonirradiation group (3 of 10 Grade 0, 3 of 10 Grade 1 and 4 of 10 Grade 2 versus 8 of 10 Grade 0 and 2 of 10 Grade 1; p = 0.04). Interobserver reliability of assessing intradural tumor invasion grades in the LM8-implanted group was 0.93. In the microstructural analysis of the dura mater using SEM, irradiated mice had small defects on the dural surface at low magnification and degeneration of collagen fibers at high magnification. The median (range) number of defects on the dural surface per image in the irradiated mice was larger than that of nonirradiated mice (2 [1 to 3] versus 0; difference of medians, 2/image; p = 0.002) and the median size of defects was 60 μm (30 to 80). Interobserver reliability of assessing number of defects on the dural surface was 1.00. TEM revealed that nonirradiated mice demonstrated well-organized, multilayer structures, while irradiated mice demonstrated irregularly layered structures at low magnification. At high magnification, well-ordered cross-sections of collagen fibers were observed in the nonirradiated mice. However, disordered alignment of collagen fibers was observed in irradiated mice.

Conclusions Intradural tumor invasion and disruptions of the dural microstructure were observed in the meninges of mice after irradiation, indicating radiation-induced disruption of the meningeal barrier.

Clinical Relevance We conclude that in this form of delivery, radiation is associated with disruption of the dural meningeal barrier, indicating a need to consider methods to avoid or limit Postradiation tumor relapse and spinal cord compression when treating spinal metastases so that patients do not experience intradural tumor invasion. Surgeons should be aware of the potential for intradural tumor invasion when they perform post-irradiation spinal surgery to minimize the risks for intraoperative dural injury and spinal cord injury. Further research in patients with irradiated spinal metastases is necessary to confirm that the same findings are observed in humans and to seek irradiation methods that prevent or minimize the disruption of meningeal barrier function.

Introduction

The number of patients in whom cancer develops is increasing worldwide [6]. Around 30% of patients with cancer will have spinal metastases and up to 20% of those patients experience paralysis resulting from spinal cord compression [10, 20, 24, 29, 37]. Paralysis caused by a spinal tumor results in poor prognosis and has a devastating impact on patients' daily activities and quality of life. However, some recent advances in cancer treatment have extended the survival period of patients with spinal metastases. One such treatment, radiotherapy, has been widely used to treat spinal metastases [30, 34] and is often performed palliatively to improve a patient's quality of life.

Long-term survivors with spinal metastases sometimes undergo surgical intervention after radiotherapy to treat recurrent pain or nerve compression because of local tumor relapse. Generally, intradural invasion of a spinal tumor rarely occurs because the dura mater serves as a tissue barrier against tumor infiltration [15]. It has been noted, however, that sometimes after irradiation, spinal tumors can invade the dura mater [18]. Intradural tumor invasion leads to leptomeningeal dissemination and causes central nervous system symptoms such as headache, vomiting, confusion, seizure, and cranial nerve palsies [35]. During surgery, intradural tumor invasion makes it difficult to dissect the tumor from the dura mater and completely resect the tumor, resulting in intraoperative dural injury or postoperative local recurrence. Intraoperative dural injury and postoperative cerebrospinal fluid leakage are frequently observed during surgery to treat spinal tumors after radiotherapy [38]; these adverse events may result in long-term bed rest and are associated with intracranial hemorrhage, increased deep wound infections or neurologic deficits such as bladder-bowel dysfunction [7, 17, 22]. A previous study confirmed that there can be epidural fibrosis and thinning of the arachnoid barrier cell layer after irradiation in mice [40]. Epidural fibrosis could be a strong risk factor for intraoperative dural injury due to peridural adhesion [39, 40]. Thinning of the arachnoid barrier cell layer, which is involved in meningeal permeability, is considered to be the cause of cerebrospinal fluid leakage despite the absence of dural injury [38, 40]. However, the mechanisms through which intradural tumor invasion occurs after irradiation remain unknown. We therefore wanted to study whether radiation exposure disrupts the barrier functions of the spinal meninges.

To investigate how radiation affects the spinal meninges, we asked: (1) What is the effect of irradiation on the meningeal barrier's ability to protect against carcinoma infiltration? (2) What is the effect of irradiation on the meningeal barrier's ability to protect against sarcoma infiltration? (3) What is the effect of irradiation on dural microstructure observed by scanning electron microscopy (SEM)? (4) What is the effect of irradiation on dural microstructure observed by transmission electron microscopy (TEM)?

Materials and Methods

Animal and Experimental Design

This study was conducted with the approval of our institutional animal care and experimentation committee (protocol number: AP-153694). All procedures were performed with the mice under sodium pentobarbital anesthesia, and all efforts were made to minimize their discomfort and suffering.

Ten-week-old female ddY mice (body mass: 30 g to 32 g) purchased from Japan SLC (Shizuoka, Japan) were used in this study. Female mice were used to model mammary tumor metastasis [19]. The ddY mice, used in the previous study investigating radiation effects on spinal dura mater [40], are closed-colony mice with genetic diversity and were selected in this study to represent interhuman diversity. All animals were maintained in a standard environment, with five mice housed per cage; mice were given free access to water and food. Animals were maintained on a 12-hour/12-hour light/dark cycle and were housed in ventilated racks with an automatic watering system.

Our primary study outcomes were to assess the incidence of intradural tumor invasion after irradiation by semiquantitative histology using tumor-induced spinal cord compression model and to assess radiation effect on dural microstructure by quantitative assessment using electron microscopy in mice.

Eighty-four mice were randomly allocated to either a 20-Gy irradiation group or a 0-Gy irradiation (non-irradiation) group. Mice in both groups underwent surgery to generate the tumor-induced spinal cord compression model at either 6 weeks or 12 weeks after

irradiation to assess changes in the meningeal barrier that protects against tumor infiltration. The lamina of the mice was exposed via a posterior approach and then intraosseous implantation of either a tumor from a mouse mammary tumor cell line (MMT; representative of a carcinoma) [32] or an osteosarcoma cell line (LM8) [1] was performed. The mice were divided into eight groups: MMT implantation 6 weeks after non-irradiation (n = 11), MMT implantation 6 weeks after irradiation (n = 10), MMT implantation 12 weeks after nonirradiation (n = 10), MMT implantation 12 weeks after irradiation (n = 11), LM8 implantation 6 weeks after nonirradiation (n = 11), LM8 implantation 6 weeks after irradiation (n = 11), LM8 implantation 12 weeks after nonirradiation (n = 10), and LM8 implantation 12 weeks after irradiation (n = 10). When the mice became paraplegic because of spinal cord compression resulting from growth of the implanted tumor, they were euthanized and evaluated histologically. Four mice died from anesthesia and 10 mice were euthanized from each of the eight groups (MMT-implanted groups included: MMT implantation 6 weeks after nonirradiation, 6 weeks after irradiation, 12 weeks after nonirradiation, and 12 weeks after irradiation; the LM8-implanted groups included: LM8 implantation 6 weeks after nonirradiation, 6 weeks after irradiation, 12 weeks after nonirradiation, and 12 weeks after irradiation), resulting in 80 specimens for histologic assessment (Fig. 1A).

Additionally, we euthanized 12 mice to assess microstructural changes in the dura mater. Six mice (three mice in the 12 weeks after nonirradiation group and three mice in the

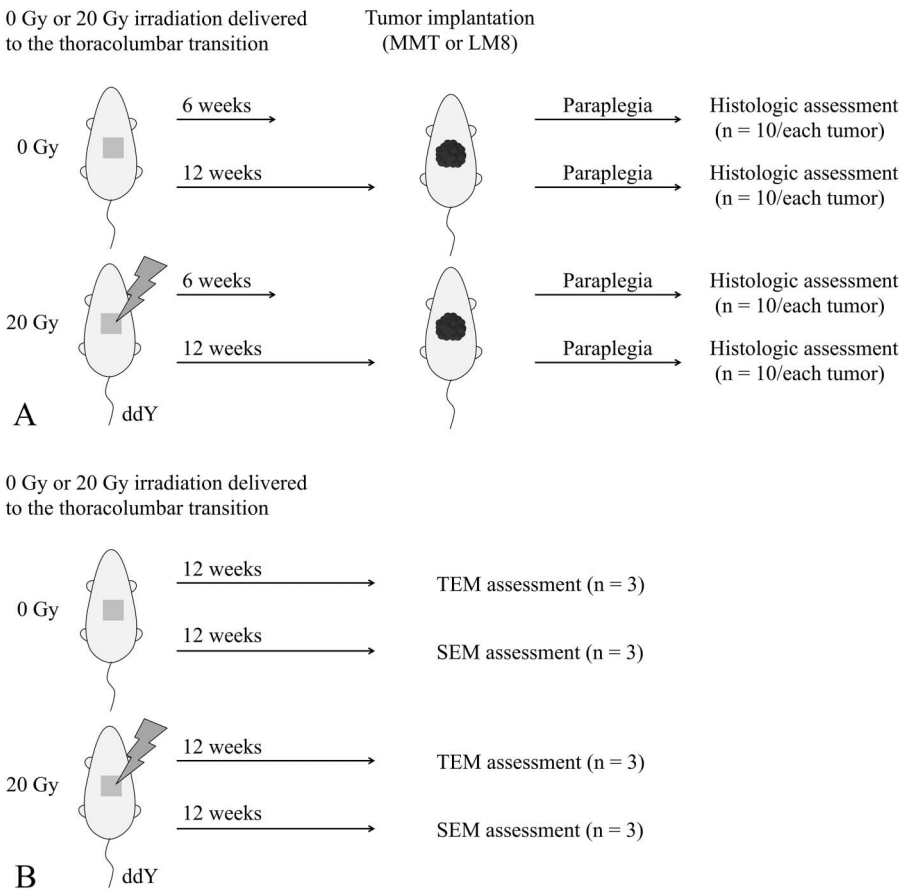

Fig. 1 A-B This diagram shows the overall experimental design. (**A**) This experiment assessed functional changes in the meningeal barrier's ability to protect against tumor infiltration by histologic assessment using tumor-induced spinal cord compression model in mice. (**B**) This experiment assessed changes in the dural microstructure after radiation exposure in mice by electron microscopy; MMT = mouse mammary tumor cells; LM8 = osteosarcoma cells; TEM = transmission electron microscopy; SEM = scanning electron microscopy.

12 weeks after irradiation group) were quantitatively analyzed by SEM and the other six mice (three mice in the 12 weeks after non-irradiation group and three mice in the 12 weeks after irradiation group) were analyzed with TEM (Fig. 1B).

Radiation Exposure

The irradiated groups received a single external 20-Gy dose of radiation (at 150 kV and 20 mA with 0.5-mm aluminum and 0.5-mm copper filters) to the thoracolumbar transition using a radiographic irradiation device for small animals (HITACHI MBR-1520R-3, Tokyo, Japan), as previously described by Yokogawa et al. [40]. After induction of general anesthesia with intraperitoneal pentobarbital (50 mg/kg), the mice were immobilized in the lateral decubitus position and irradiated under a lead shield with a 20-mm × 20-mm window to restrict irradiation to the thoracolumbar transition alone. The non-irradiation groups underwent sham procedures that involved the same anesthesia protocol but without radiation exposure. The 20-Gy dose used in this study was previously determined to be biologically equivalent to the dose generally used in single-fraction palliative radiotherapy in humans [8, 21].

Tumor Cell Lines

We used the MMT and LM8 cell lines in this study. We selected MMT because it represents spinal metastatic carcinomas, and we used LM8 to represent sarcomas. All MMT and LM8 cells were cultured in Dulbecco's modified Eagle's medium supplemented with 5% fetal bovine serum, penicillin (100 U/mL), and streptomycin (100 μg/mL at 37° C). Cultures were maintained in 5% CO_2 at 37° C.

We used a subcutaneous tumor as the source of the solid tumor grafts. The mice were anesthetized with intraperitoneal pentobarbital (50 mg/kg) and received a subcutaneous injection of a solution containing $15^6 \times 10^6$ MMT or LM8 cells in the left hind limb. On Day 12 post-injection, the animals were euthanized, and the tumors were resected and sliced into 0.3 cm × 0.3 cm pieces for implantation.

Surgical Procedures to Generate the Tumor-induced Spinal Cord Compression Model

Both the irradiation and the nonirradiation groups underwent surgery to generate the tumor-induced spinal cord compression model at either 6 weeks or 12 weeks post-irradiation. The surgery was performed in mice based on the procedure developed by Zibly et al. [41]. After anesthesia with intraperitoneal pentobarbital (50 mg/kg), the animal was placed in the prone position. A 3-cm midline skin incision was made above the spinal process of the irradiated thoracolumbar transition and a skin retractor was used. A subperiosteal, blunt dissection of the spinalis muscle was performed bilaterally to expose the lamina. The spinous process and outer cortex of the lamina were drilled, leaving the internal cortex intact (Fig. 2A). A fragment of the MMT or LM8 tumor was implanted at the residual internal cortex of the lamina (Fig. 2B). The dorsal fascia was closed tightly using an interrupted 3-0 Vicryl suture. The skin was closed with a running 4-0 nylon suture. After surgery, the animals were examined daily for assessment of hind limb motor function by a single investigator (MH) blinded to the type of tumor, presence of irradiation, and the timing of the surgery after irradiation. When the animals experienced complete paraplegia because of spinal

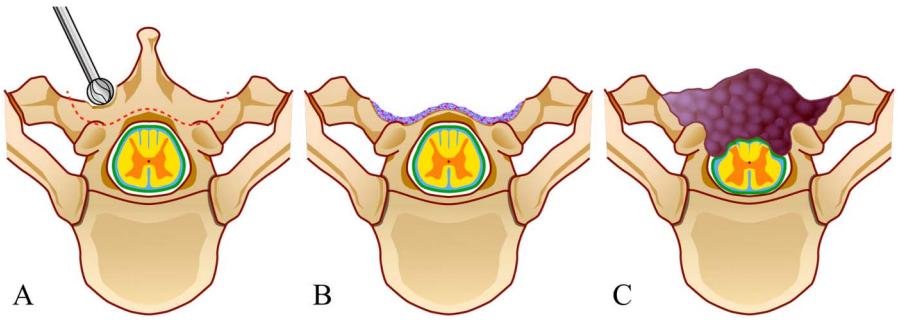

Fig. 2 A-C These illustrations show the surgical procedure for the mouse model of tumor-induced spinal cord compression. (**A**) After high-speed drilling of the spinous process and outer cortex of the lamina, the internal cortex was left intact. (**B**) The tumor was implanted at the residual internal cortex of the lamina. (**C**) The implanted tumor grows and penetrates the internal cortex of the lamina, compressing the spinal cord and ultimately results in paraplegia. Published with permission from Toshyia Nomura.

cord compression resulting from growth of the implanted tumor (Fig. 2C), they were euthanized with intraperitoneal pentobarbital (150 mg/kg) and subsequently perfused with 4% paraformaldehyde/0.1 M phosphate buffer solution (Ph 7.4). Subsequent en-bloc excision of the spines was performed, and the specimens were histologically assessed. All irradiated mice developed radiation dermatitis in the irradiated skin. There were no surgical complications, and all mice survived the procedure and developed the predicted paraplegia.

Histologic Assessment

For the histologic assessment, the excised specimens were fixed in Tissue-Tek UFIX (Sakura Finetek Japan, Tokyo, Japan) for 3 days and decalcified with 10% formic acid for 1 week. Interlaminar horizontal sections of the resected specimens were embedded in paraffin and cut into 2-μm sections for hematoxylin and eosin staining and Masson's trichrome staining. The section demonstrating the most extensively destructed inner cortex of the lamina was

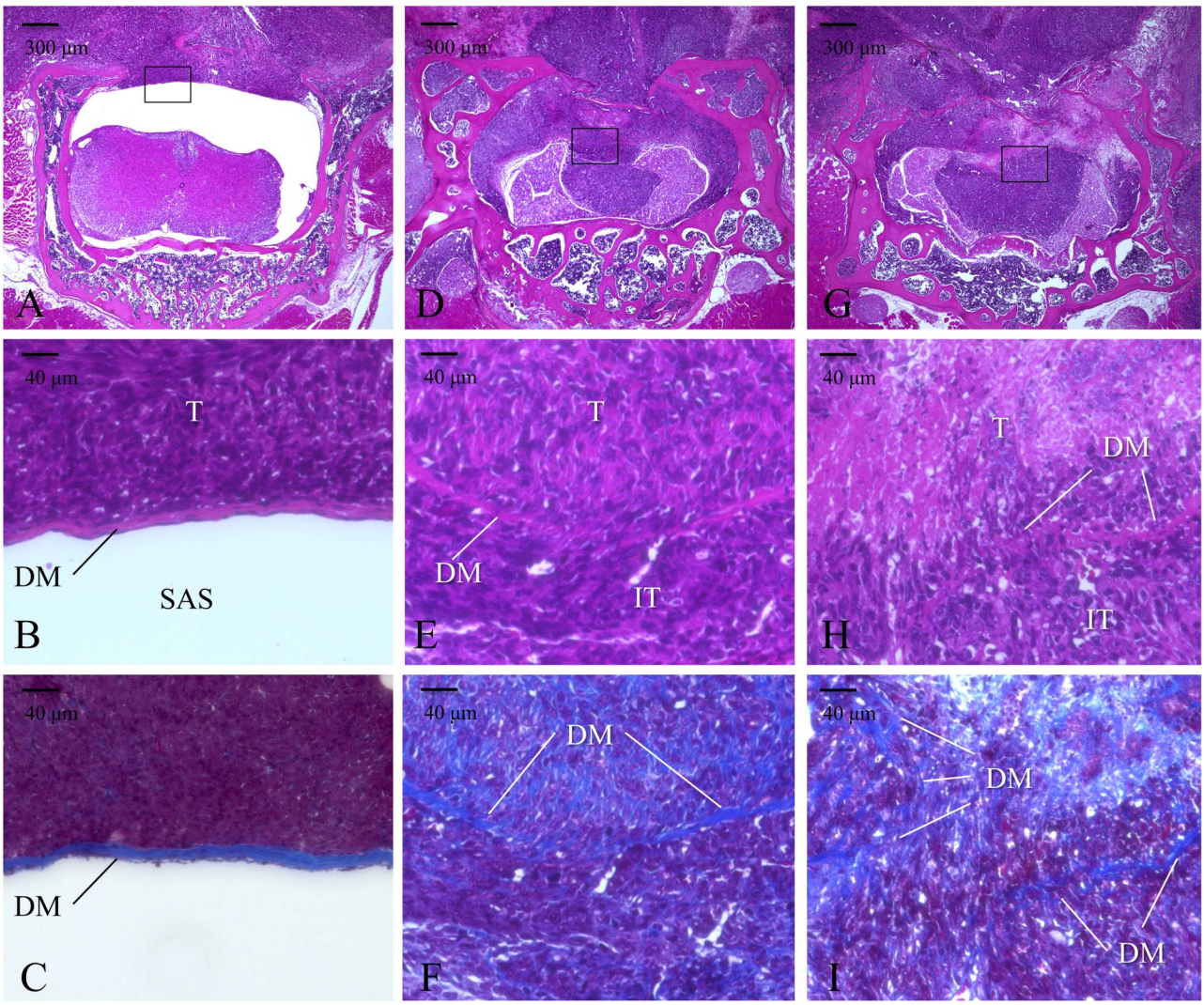

Fig. 3 A-I These histologic images represent each grade of intradural tumor invasion. (**A**) This hematoxylin and eosin (HE) staining shows Grade 0 at low magnification (scale bars = 300 μm). (**B**) HE staining of Grade 0 shows no intradural invasion at high magnification (scale bars = 40 μm). (**C**) Masson's trichrome (MT) staining of Grade 0 shows completely intact dura mater at high magnification (scale bars = 40 μm). (**D**) HE staining of Grade 1 at low magnification (scale bars = 300 μm) is shown. (**E**) HE staining of Grade 1 shows intradural invasion at high magnification (scale bars = 40 μm). (**F**) MT staining of Grade 1 shows linear dural continuity at high magnification (scale bars = 40 μm). (**G**) This HE staining shows Grade 2 at low magnification (scale bars = 300 μm). (**H**) HE staining of Grade 2 shows intradural invasion at high magnification (scale bars = 40 μm). (**I**) MT staining of Grade 2 shows disrupted dural continuity at high magnification (scale bars = 40 μm); T = tumor; DM = dura mater; SAS = subarachnoid space; IT = invaded tumor beyond the dura mater.

evaluated using a BZ-9000 microscope (Keyence, Osaka, Japan). Three observers (TS, SD, TN) blinded to the type of tumor, presence of irradiation, and the timing of the surgery after irradiation independently graded the intradural invasion of the tumors from 0 (no intradural invasion) to 2 (severe intradural invasion). Grade 0 was defined as no intradural invasion with intact dura mater, Grade 1 was defined as intradural invasion with linear dural continuity, and Grade 2 was defined as intradural invasion with disruption of the dural continuity. Hematoxylin and eosin staining was evaluated for intradural tumor invasion and Masson's trichrome staining was used for evaluation of dural continuity (Fig. 3A-I). The median value of the intradural invasion grade was considered the intradural invasion grade of the specimen.

Microstructural Assessment

For the SEM assessment, the excised spinal cords were fixed with 2% paraformaldehyde and 2% glutaraldehyde at 4° C overnight and fixed with 1% tannic acid at 4° C for 2 hours. After post-fixation with 2% osmium tetroxide at 4° C for 3 hours, the samples were dehydrated in graded ethanol solutions. The solutions containing the samples were substituted with tert-butyl alcohol, followed by freezing of the samples at 4° C. The frozen samples were vacuum-dried and coated with a thin layer (50-nm) of osmium using an osmium plasma coater (NL-OPC80A; Nippon Laser & Electronics Laboratory, Nagoya, Japan). The samples were assessed using an SEM (JSM-7500F; JEOL Ltd., Tokyo, Japan) to assess microstructural changes.

In the SEM assessment, two observers (TS, TN) blinded to the presence of irradiation independently evaluated the number and size of defects on the dural surface on images (200 μm × 300 μm) at low magnification (× 2680). A total of 12 images (two images from each six mice) were evaluated for this assessment. The mean value of the number and size of defects on the dural surface was considered the number and size of defects of the specimen.

For the TEM assessment, the excised spinal cords were fixed with 2% paraformaldehyde and 2% glutaraldehyde in 0.1 M cacodylate buffer pH 7.4 at 4° C overnight, then post-fixed with 2% osmium tetroxide at 4° C for 3 hours. The samples were dehydrated in graded ethanol solutions. The samples were then infiltrated with propyleneoxide and were put into a 70:30 mixture of propyleneoxide and resin (Quetol-812; Nisshin EM Co, Tokyo, Japan) for l hour. The samples were transferred to fresh 100% resin and allowed to polymerize at 60° C for 48 hours. The polymerized resin blocks underwent ultra-thin sectioning at a 70-nm thickness using an ultra-microtome. Samples were stained with 2% uranylacetate and lead citrate and assessed using a transmission electron microscope (JEM-1400Plus; JEOL Ltd., Tokyo, Japan).

Statistical Analyses

The days from surgery to paraplegia are expressed as the median (range) and were compared between each of the tumor groups using the Kruskal-Wallis test. We compared the scores of intradural tumor invasion grades and the number of defects on the dural surface per SEM image between the irradiation group and the nonirradiation group

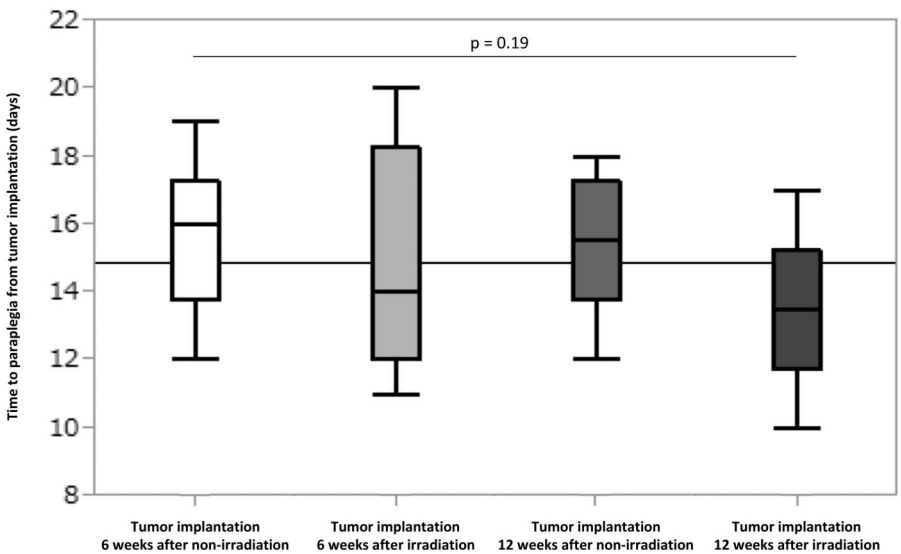

Fig. 4 This whisker plot shows the time to paraplegia from tumor implantation in each mouse mammary tumor-implanted group. There was no difference in the time to paraplegia among groups.

using the Mann-Whitney U test. Interobserver reliabilities of assessing intradural tumor invasion grades and the number of dural defects on the dural surface were analyzed using Fleiss'κ coefficient. P values < 0.05 were considered statistically significant. All statistical analyses were performed using R Software for Statistical Computing (version 2.8.1; R Foundation for Statistical Computing, Vienna, Austria).

Results

The Effect of Irradiation on the Meningeal Barrier's Ability to Protect Against Carcinoma Infiltration

There was no difference in the median (range) time to paraplegia among the MMT implantation 6 weeks after nonirradiation group, the 6 weeks after irradiation group, the 12 weeks after nonirradiation group, and the 12 weeks after irradiation group (16 days [14 to 17] versus 14 days [12 to 18] versus 16 days [14 to 17] versus 14 days [12 to 15]; χ^2 = 4.7; p = 0.19) (Fig. 4). In the MMT-implanted groups, there was no difference in the intradural invasion score between the MMT implantation 6 weeks after irradiation group and the 6 weeks after nonirradiation group (8 of 10 Grade 0 and 2 of 10 Grade 1 versus 10 of 10 Grade 0; p = 0.17). On the other hand, there was a higher intradural invasion score in the MMT implantation 12 weeks after irradiation group than 12 weeks after nonirradiation group (5 of 10 Grade 0, 3 of 10 Grade 1 and 2 of 10 Grade 2 versus 10 of 10 Grade 0; p = 0.02) (Fig. 5). An analysis of interobserver reliability showed that the Fleiss' κ coefficient for assessing intradural tumor invasion grades was 0.94.

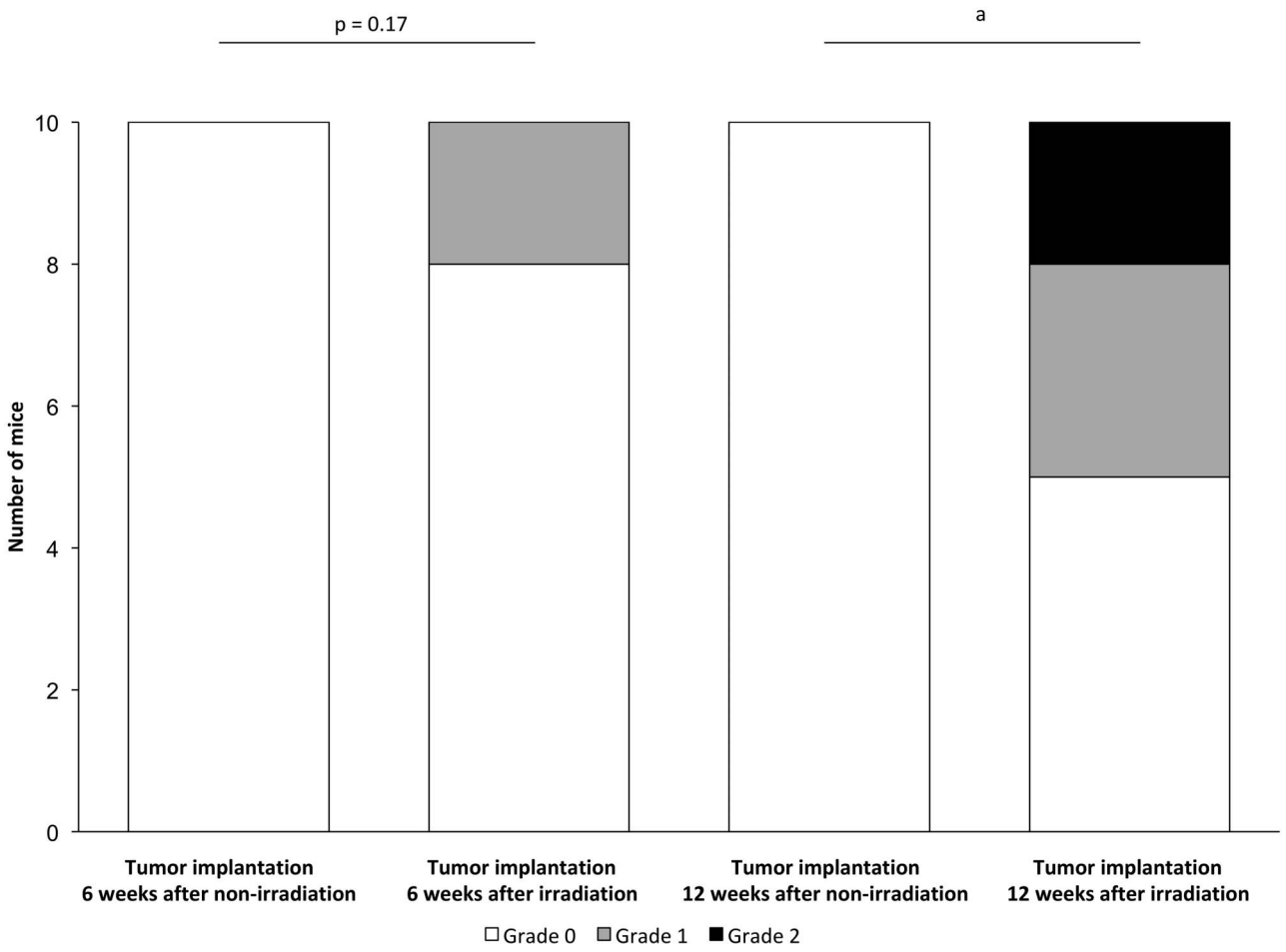

Fig. 5 This 100% stacked histogram shows distribution of intradural invasion grades in each mouse mammary tumor (MMT)-implanted group. There was no difference in the intradural invasion score between the MMT implantation 6 weeks after non-irradiation group and the 6 weeks after irradiation group. There was a higher intradural invasion score in the MMT implantation 12 weeks after irradiation group than in the 12 weeks after nonirradiation group.[a]Indicates a difference between groups at the p < 0.05 level.

The Effect of Irradiation on the Meningeal Barrier's Ability to Protect Against Sarcoma Infiltration

There was no difference in the median (range) time to paraplegia among the LM8 implantation 6 weeks after non-irradiation group, the 6 weeks after irradiation group, the 12 weeks after nonirradiation group, and the 12 weeks after irradiation group (12 days [9 to 13] versus 10 days [8 to 13] versus 11 days [8 to 13] versus 9 days [6 to 12]; $\chi^2 = 2.4$; $p = 0.50$) (Fig. 6). In the LM8-implanted groups, there was no difference in the intradural invasion score between the LM8 implantation 6 weeks after irradiation group and the 6 weeks after nonirradiation group (7 of 10 Grade 0, 1 of 10 Grade 1 and 2 of 10 Grade 2 versus 8 of 10 Grade 0 and 2 of 10 Grade 1; $p = 0.51$). In contrast, there was a higher intradural invasion score in the LM8 implantation 12 weeks after irradiation group than in the 12 weeks after nonirradiation group (3 of 10 Grade 0, 3 of 10 Grade 1 and 4 of 10 Grade 2 versus 8 of 10 Grade 0 and 2 of 10 Grade 1; $p = 0.04$) (Fig. 7). An analysis of interobserver reliability showed that Fleiss' κ coefficients for assessing intradural tumor invasion grades was 0.93.

The Effects of Irradiation on Dural Microstructure Observed by SEM

In the SEM analysis, non-irradiated mice demonstrated packed surface of the dura mater, while irradiated mice exhibited small defects on the dural surface that were visible at low magnification (× 2680). The beaded structure of collagen fibers constituting the dural surface was observed in nonirradiated mice at high magnification (× 13,400) while degeneration of collagen fibers was observed in irradiation mice (Fig. 8A-D). The median (range) number of defects on the dural surface per image in the irradiated mice was larger than that of nonirradiated mice (2 [1 to 3] versus 0; difference of medians, 2/image; $p = 0.002$) and the median size of defects was 60 μm (30 to 80). An analysis of interobserver reliability showed that Fleiss' κ coefficients for assessing number of defects on the dural surface was 1.00.

The Effects of Irradiation on Dural Microstructure Observed by TEM

In the microstructural analysis of the dura mater using TEM, nonirradiated mice demonstrated well-organized, multilayered structures of collagen fibers with interspersed fibrocytes, while irradiated mice demonstrated irregularly structured layers of collagen fibers with interspersed fibrocytes at low magnification (× 4210). At high magnification (× 21,100), well-ordered collagen fiber cross-sections were observed in the nonirradiated mice, while irradiated mice exhibited disordered alignment of collagen fibers (Fig. 9A-D).

Discussion

Treatment of spinal metastases requires consideration of numerous factors, including the patient's general

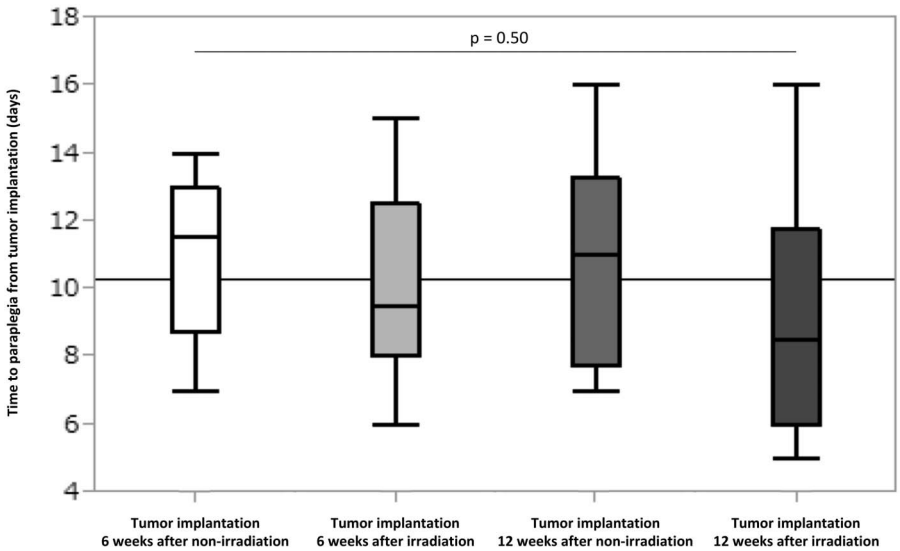

Fig. 6 This whisker plot shows the time to paraplegia from tumor implantation in each LM8 mouse osteosarcoma cell line-implanted group. There was no difference in the time to paraplegia among groups.

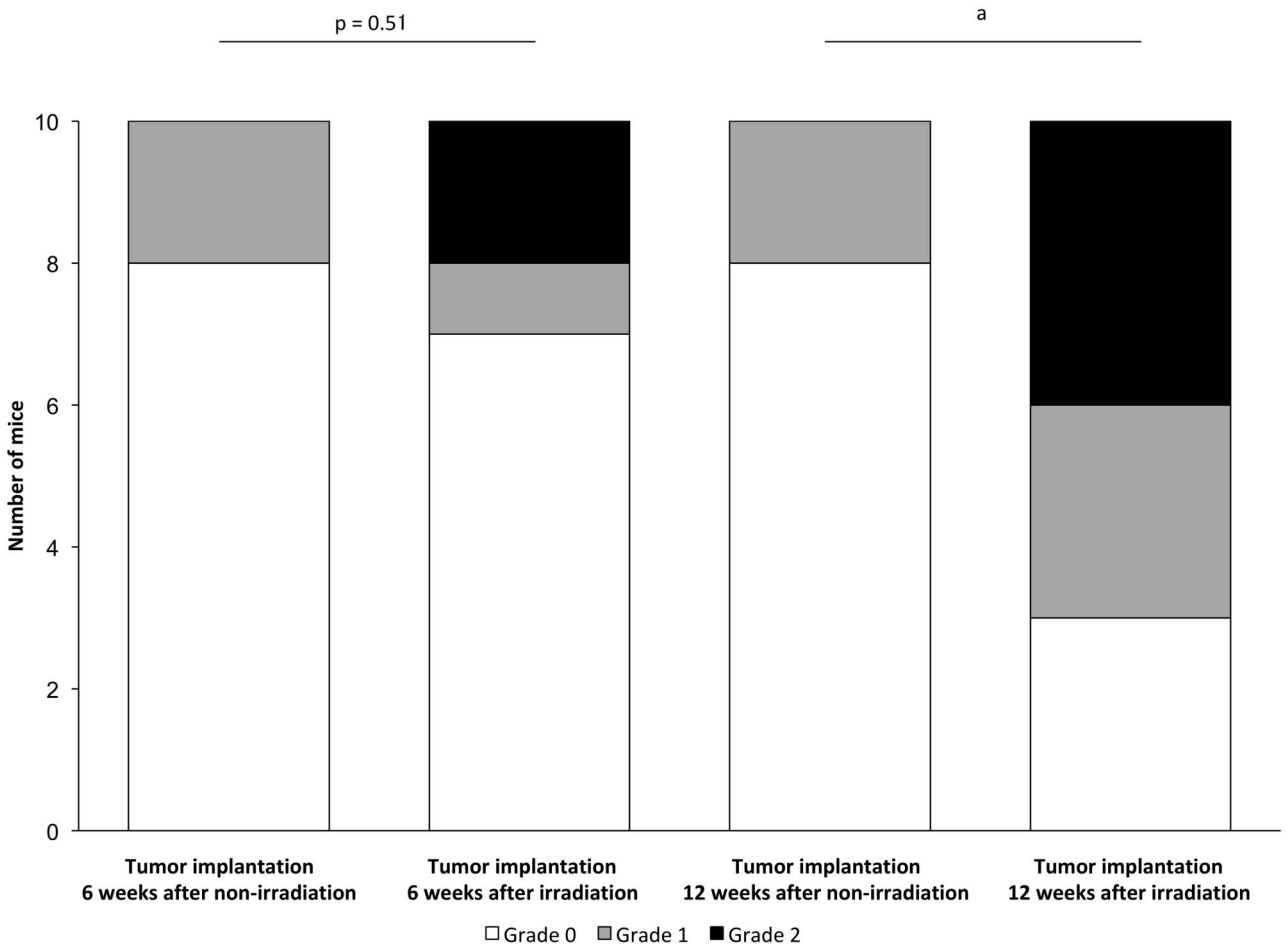

Fig. 7 This 100% stacked histogram shows distribution of intradural invasion grades in each LM8 implanted group. There was no difference in the intradural invasion score between LM8 mouse osteosarcoma cell line implantation at 6 weeks in the nonirradiation group and 6 weeks in the irradiation group. There was a higher intradural invasion score in the LM8 implantation 12 weeks after irradiation group than the 12 weeks after non-irradiation group. [a]Indicates a difference between groups at the $p < 0.05$ level.

condition, prognosis, type of tumor, response to prior therapy, location where the spine is affected, mechanical instability, and other neurologic factors. In a recent review, radiation therapy was identified as the main means to manage spinal metastases [30]. However, cautious consideration of these factors is required to avoid spinal surgery in patients with tumor relapse after irradiation because prior radiotherapy is associated with an increased risk of surgical complications such as wound dehiscence, deep infection, and dural injury and subsequent cerebrospinal fluid leakage [11, 14, 16, 25, 27, 31, 36, 38]. In this study, we investigated the postirradiation changes that occurred in spinal meninges and found there was disruption to the protective meningeal barrier function after irradiation, as evidenced by increased intradural tumor invasion in a tumor-induced spinal cord compression model, as well as disruption of the microstructure of the dura mater. The results of this study indicate that patients with irradiated spinal metastases have the potential develop intradural tumor invasion. Knowledge of this phenomenon make essential to attempt to avoid postirradiation tumor relapse and spinal cord compression so that patients do not experience intradural invasion.

Limitations

This study had several limitations. First, and most importantly, this study was performed in mice. As with all murine studies, there are limitations in extrapolating findings to humans. However, given that various murine studies analyzing radiation-induced normal tissue reaction have been widely conducted and have led to important findings for humans [12, 13, 21, 40], we believe the results of this study

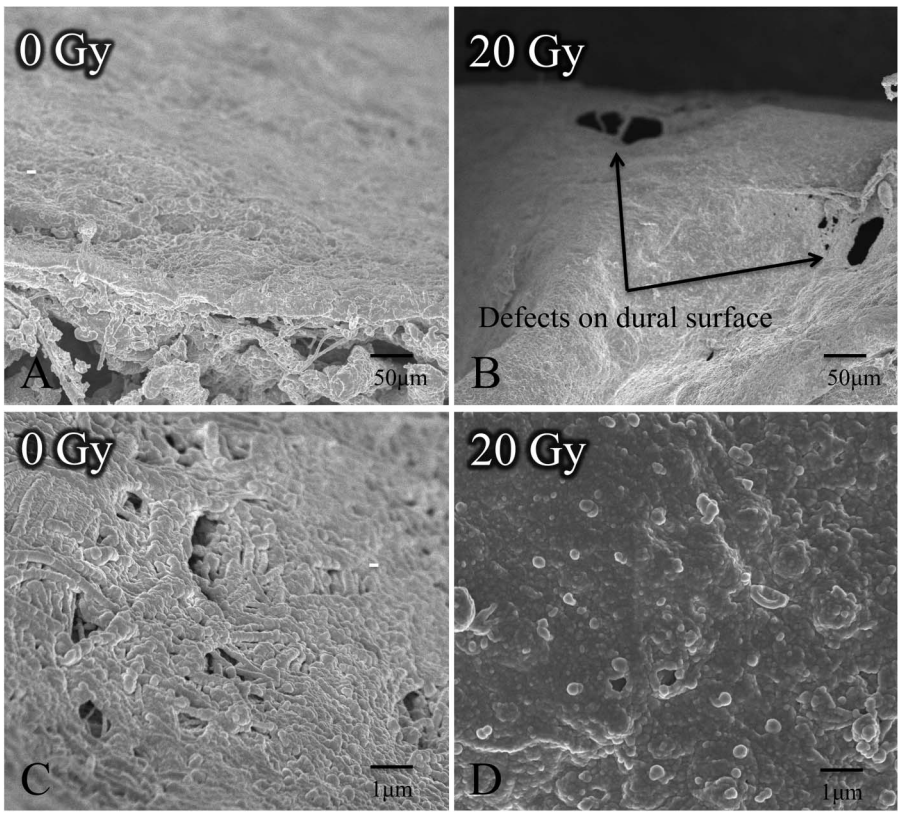

Fig. 8 A-D These images show the dural surface observed by scanning electron microscopy. (**A**) The nonirradiated group demonstrated packed surface without defect in the dura at low magnification (scale bars = 50 μm). (**B**) The irradiated group demonstrated defects on the surface of the dura at low magnification (scale bars = 50 μm). (**C**) The nonirradiated group showed beaded structure of collagen fiber at high magnification (scale bars = 1 μm). (**D**) The beaded structure of collagen fiber is shredded in the irradiated group (scale bars = 1 μm); 0 Gy = nonirradiated group; 20 Gy = irradiated group.

can contribute to the elucidation of the radiation effects on human meninges. Second, single-fraction radiotherapy was used to irradiate tissue because it was technically difficult to perform multiple-fraction radiotherapy repeatedly at the same area of the spine in mice. In addition, surgery must be performed at the very place where radiation was performed. Fractionated radiation was considered to complicate the experiment and reduce accuracy, so single-fraction radiation was selected in this study. Although fractionated, long-course radiotherapy is associated with better local control and is widely used to manage spinal metastases, there is no difference in acute and late adverse events between single and fractionated irradiation for bone metastases [9, 28]. Therefore, multifraction radiotherapy is unlikey to produce completely different results from this study. Finally, in this study, the tumors were implanted after irradiation, which differs from what occurs clinically; in clinical practice, of course, radiation is delivered to where the tumor is located. This is an inherent limitation of the model because irradiation shrinks the tumor after implantation, making it difficult to generate a tumor-induced spinal cord compression model. However, this model differs from clinical practice in lacking the process of temporary tumor shrinkage after irradiation, but this limitation does not disqualify the results of the experiment.

Intradural Invasion Increased After Radiation

In our experiment using the tumor-induced spinal cord compression model to investigate changes in the meningeal barrier's ability to protect against tumor infiltration, intradural tumor invasion was increased in the irradiated groups, which supports our contention that radiation exposure disrupts the barrier function of the meninges. In addition, among the nonirradiated mice, two LM8-implanted mice exhibited intradural invasion, while none was observed in the MMT-implanted mice. These differences are likely

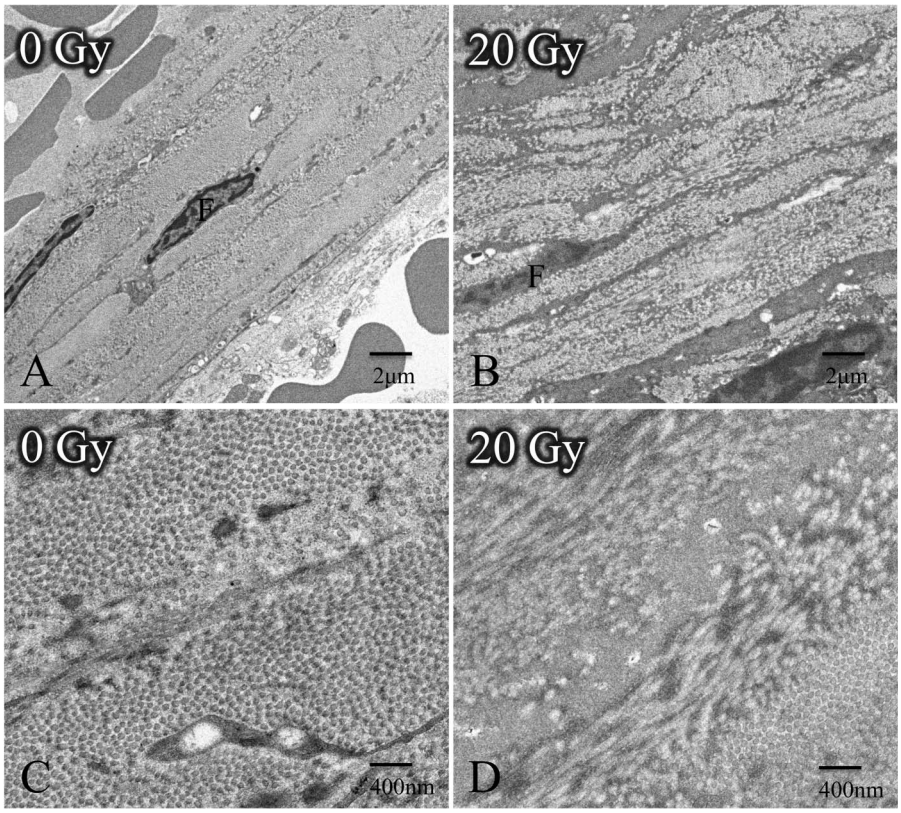

Fig. 9 A-D These images show the cross-section of dura mater observed by transmission electron microscopy. (**A**) The non-irradiation group demonstrated well-organized, linear multilayered structures of collagen fibers with interspersed fibrocytes at low magnification (scale bars = 2 μm). (**B**) The irradiation group demonstrated waved, irregularly structured layers of collagen fibers with interspersed fibrocytes at low magnification (scale bars = 2 μm). (**C**) The nonirradiation group showed cross-sections of well-ordered collagen fibers at high magnification (scale bars = 400 nm). (**D**) Some collagen fibers are perpendicular to the cross-section surface while some fibers are parallel or diagonal in the irradiation group at high magnification (scale bars = 400 nm); 0 Gy = nonirradiation group; F = fibrocyte; 20 Gy = irradiated group; Cf = collagen fiber.

because of differences in the invasive features of each tumor type. The dura mater acts as the outermost tissue barrier of the meninges to prevent tumors from spreading locally [23]. Some highly malignant tumors, such as osteosarcomas, can destroy and invade the dura mater [23]. LM8, the murine osteosarcoma cell line used in the current study, exhibits highly invasive activity and has high metastatic potential [1]. These characteristics of LM8 likely explain the greater intradural invasion than in MMT tumors.

Radiation Causes Structural Changes to the Dura Mater

Our microstructural analysis using electron microscopy showed degeneration and disordered alignment of collagen fibers of the dura mater and small defects of the dural surface in the irradiated mice. Although the exact mechanism responsible for these radiation-induced changes in collagen structure is unknown, irradiation causes fragmentation and nonenzymatic crosslinking of collagen molecules, resulting in decreased mechanical strength [2-4, 26]. Therefore, irradiated dura is considered to lose mechanical strength due to decreased mechanical strength of irradiated collagens [2-4, 26] of which dura are made. Furthermore, irradiated dura has surface defects. These two changes in irradiated dura indicate disruption of the mechanical barrier of the meninges. Additionally, a previous report showed thinning of the arachnoid barrier cell layer, which is constituted of cells with tight junctions and located in the outermost layer of the arachnoid mater [33], in the late stages after irradiation [40]. This indicates

disruption of the chemical barrier of the meninges because the arachnoid barrier's cell layer is strongly associated with meningeal permeability [5]. Therefore, irradiation may disrupt the meninges' ability to act as a barrier against mechanical and chemical damage, which may explain intradural invasion of spinal tumors and cerebrospinal fluid leakage after surgery in patients who undergo irradiation.

Potential Clinical Relevance and Next Steps

The results of this study show that intradural invasion of a spinal tumor may occur in mice that receive irradiation and are subsequently implanted with a tumor; this complication is likely the result of disruption of the dural structure. If the findings we observed in mice occur in humans, patients with spinal tumors treated with irradiation may survive and experience tumor recurrences that invade the meninges because the meningeal barrier function that protects against tumor infiltration becomes disrupted after radiation therapy (at least in mice). Tumor invasion into the meninges contributes to leptomeningeal dissemination or dural injuries during surgery, resulting in devastating prognoses. Therefore, we have to make the best effort to avoid postirradiation tumor relapse, for example, we should consider surgical intervention before radiotherapy for tumors with low radiosensitivity and long-term prognosis. We need postmortem research in patients with postirradiation spinal metastases to confirm whether the same findings are observed in humans and identify the irradiation methods that prevent or reduce the disruption of the meningeal barrier function. To avoid postirradiation tumor relapse and spinal cord compression, it is also necessary to determine which patients can be effectively treated with radiation therapy alone and which patients must undergo surgical intervention first. A further study of a large-scale dataset is necessary to establish more-classified treatment algorithms for spinal metastases that can prevent or reduce the need for further postirradiation spinal surgery.

Conclusions

In summary, we observed intradural tumor invasion and disruption of the dural microstructure in the meninges of mice after irradiation, indicating disruption of the protective barrier functions of the meninges after radiation therapy to treat spinal tumors. If confirmed in the human dural structures, we should consider methods to avoid or lessen the likelihood of tumor relapse in patients who have undergone irradiation when treating spinal metastases so they do not experience intradural tumor invasion. In addition, surgeons should be aware of the potential for intradural tumor invasion, which poses a surgical challenge when they perform postirradiation spinal surgery to minimize the risks for intraoperative dural injury and spinal cord injury. Research in patients with irradiated spinal metastases is necessary to confirm whether similar findings are observed in humans and seek the irradiation method that reduces adverse changes in the dura after irradiation of the spinal column.

Acknowledgments We thank Ms. Yoko Kasai at the Department of Orthopaedic Surgery, Graduate School of Medical Sciences, Kanazawa University, Kanazawa, Japan, for her skillful technical assistance on the histology. We thank Editage (www.editage.com) for English-language editing.

References

1. Asai T, Ueda T, Itoh K, Yoshioka K, Aoki Y, Mori S, Yoshikawa H. Establishment and characterization of a murine osteosarcoma cell line (LM8) with high metastatic potential to the lung. *Int J Cancer*. 1998;76:418-422.
2. Bailey AJ, Rhodes DN, Cater CW. Irradiation-induced cross-linking of collagen. *Radiat Res*. 1964;22:606-621.
3. Barth HD, Launey ME, Macdowell AA, Ager JW 3rd, Ritchie RO. On the effect of X-ray irradiation on the deformation and fracture behavior of human cortical bone. *Bone*. 2010;46:1475-1485.
4. Barth HD, Zimmermann EA, Schaible E, Tang SY, Alliston T, Ritchie RO. Characterization of the effects of x-ray irradiation on the hierarchical structure and mechanical properties of human cortical bone. *Biomaterials*. 2011;32:8892-8904.
5. Bernards CM, Hill HF. Morphine and alfentanil permeability through the spinal dura, arachnoid, and pia mater of dogs and monkeys. *Anesthesiology*. 1990;73:1214-1219.
6. Bray F, Ferlay J, Soerjomataram I, Siegel RL, Torre LA, Jemal A. Global cancer statistics 2018: GLOBOCAN estimates of incidence and mortality worldwide for 36 cancers in 185 countries. *CA Cancer J Clin*. 2018;68:394-424.
7. Cammisa FP Jr., Girardi FP, Sangani PK, Parvataneni HK, Cadag S, Sandhu HS. Incidental durotomy in spine surgery. *Spine (Phila Pa* 1976). 2000;25:2663-2667.
8. Chow E, Harris K, Fan G, Tsao M, Sze WM. Palliative radiotherapy trials for bone metastases: a systematic review. *J Clin Oncol*. 2007;25:1423-1436.
9. Chow E, Zeng L, Salvo N, Dennis K, Tsao M, Lutz S. Update on the systematic review of palliative radiotherapy trials for bone metastases. *Clin Oncol (R Coll Radiol)*. 2012;24:112-124.
10. Cobb CA 3rd, Leavens ME, Eckles N. Indications for nonoperative treatment of spinal cord compression due to breast cancer. *J Neurosurg*. 1977;47:653-658.
11. Demura S, Kawahara N, Murakami H, Nambu K, Kato S, Yoshioka K, Okayama T, Tomita K. Surgical site infection in spinal metastasis: risk factors and countermeasures. *Spine (Phila Pa 1976)*. 2009;34:635-639.
12. Douglas BG, Fowler JF. The effect of multiple small doses of X rays on skin reactions in the mouse and a basic interpretation. 1976. *Radiat Res*. 2012;178:AV125-138.
13. Du M, Irani RA, Stivers DN, Lee SJ, Travis EL. H2-Ea deficiency is a risk factor for bleomycin-induced lung fibrosis in mice. *Cancer Res*. 2004;64:6835-6839.
14. Fourney DR, Abi-Said D, Lang FF, McCutcheon IE, Gokaslan ZL. Use of pedicle screw fixation in the management of

malignant spinal disease: experience in 100 consecutive procedures. *J Neurosurg*. 2001;94:25-37.
15. Fujita T, Ueda Y, Kawahara N, Baba H, Tomita K. Local spread of metastatic vertebral tumors. A histologic study. *Spine (Phila Pa 1976)*. 1997;22:1905-1912.
16. Ghogawala Z, Mansfield FL, Borges LF. Spinal radiation before surgical decompression adversely affects outcomes of surgery for symptomatic metastatic spinal cord compression. *Spine (Phila Pa 1976)*. 2001;26:818-824.
17. Goodkin R, Laska LL. Unintended "incidental" durotomy during surgery of the lumbar spine: medicolegal implications. *Surg Neurol*. 1995;43:4-12; discussion 12-14.
18. Igarashi T, Murakami H, Demura S, Kato S, Yoshioka K, Yokogawa N, Tsuchiya H. Risk factors for local recurrence after total en bloc spondylectomy for metastatic spinal tumors: A retrospective study. *J Orthop Sci*. 2018;23:459-463.
19. Jonkers J, Derksen PW. Modeling metastatic breast cancer in mice. *J Mammary Gland Biol Neoplasia*. 2007;12:191-203.
20. Kakhki VR, Anvari K, Sadeghi R, Mahmoudian AS, Torabian-Kakhki M. Pattern and distribution of bone metastases in common malignant tumors. *Nucl Med Rev Cent East Eur*. 2013;16: 66-69.
21. Lo Y, Taylor JM, McBride WH, Withers HR. The effect of fractionated doses of radiation on mouse spinal cord. *Int J Radiat Oncol Biol Phys*. 1993;27:309-317.
22. Morimoto T, Shiraki M, Otani K, Sonohata M, Mawatari M. Supratentorial subdural hemorrhage of a previous head injury and cerebellar hemorrhage after cervical spinal surgery: a case report and review of the literature. *Spine (Phila Pa 1976)*. 2014; 39:E743-747.
23. Murakami H, Kawahara N, Tsuchiya H, Demura S, Yamaguchi T, Tomita K. Invasive features of spinal osteosarcoma obtained from whole-mount sections of total en bloc spondylectomy. *J Orthop Sci*. 2007;12:311-315.
24. Ortiz Gomez JA. The incidence of vertebral body metastases. *Int Orthop*. 1995;19:309-311.
25. Pascal-Moussellard H, Broc G, Pointillart V, Simeon F, Vital JM, Senegas J. Complications of vertebral metastasis surgery. *Eur Spine J*. 1998;7:438-444.
26. Pendleton MM, Emerzian SR, Liu J, Tang SY, O'Connell GD, Alwood JS, Keaveny TM. Effects of ex vivo ionizing radiation on collagen structure and whole-bone mechanical properties of mouse vertebrae. *Bone*. 2019;128:115043.
27. Quan GM, Vital JM, Aurouer N, Obeid I, Palussiere J, Diallo A, Pointillart V. Surgery improves pain, function and quality of life in patients with spinal metastases: a prospective study on 118 patients. *Eur Spine J*. 2011;20:1970-1978.
28. Rades D, Lange M, Veninga T, Stalpers LJ, Bajrovic A, Adamietz IA, Rudat V, Schild SE. Final results of a prospective study comparing the local control of short-course and long-course radiotherapy for metastatic spinal cord compression. *Int J Radiat Oncol Biol Phys*. 2011;79:524-530.
29. Schaberg J, Gainor BJ. A profile of metastatic carcinoma of the spine. *Spine (Phila Pa 1976)*. 1985;10:19-20.
30. Spratt DE, Beeler WH, de Moraes FY, Rhines LD, Gemmete JJ, Chaudhary N, Shultz DB, Smith SR, Berlin A, Dahele M, Slotman BJ, Younge KC, Bilsky M, Park P, Szerlip NJ. An integrated multidisciplinary algorithm for the management of spinal metastases: an International Spine Oncology Consortium report. *Lancet Oncol*. 2017;18:e720-e730.
31. Sundaresan N, Rothman A, Manhart K, Kelliher K. Surgery for solitary metastases of the spine: rationale and results of treatment. *Spine (Phila Pa 1976)*. 2002;27:1802-1806.
32. Sykes JA, Whitescarver J, Briggs L. Observations on a cell line producing mammary tumor virus. *J Natl Cancer Inst*. 1968;41: 1315-1327.
33. Vandenabeele F, Creemers J, Lambrichts I. Ultrastructure of the human spinal arachnoid mater and dura mater. *J Anat*. 1996;189(Pt 2):417-430.
34. Vellayappan BA, Chao ST, Foote M, Guckenberger M, Redmond KJ, Chang EL, Mayr NA, Sahgal A, Lo SS. The evolution and rise of stereotactic body radiotherapy (SBRT) for spinal metastases. *Expert Rev Anticancer Ther*. 2018;18: 887-900.
35. Wang N, Bertalan MS, Brastianos PK. Leptomeningeal metastasis from systemic cancer: Review and update on management. *Cancer*. 2018;124:21-35.
36. Wise JJ, Fischgrund JS, Herkowitz HN, Montgomery D, Kurz LT. Complication, survival rates, and risk factors of surgery for metastatic disease of the spine. *Spine (Phila Pa1976)*. 1999;24: 1943-1951.
37. Wong DA, Fornasier VL, MacNab I. Spinal metastases: the obvious, the occult, and the impostors. *Spine (Phila Pa 1976)*. 1990; 15:1-4.
38. Yokogawa N, Murakami H, Demura S, Kato S, Yoshioka K, Hayashi H, Ishii T, Igarashi T, Fang X, Tsuchiya H. Perioperative complications of total en bloc spondylectomy: adverse effects of preoperative irradiation. *PLoS One*. 2014;9:e98797.
39. Yokogawa N, Murakami H, Demura S, Kato S, Yoshioka K, Tsuchiya H. Incidental durotomy during total en bloc spondylectomy. *Spine J*. 2018;18:381-386.
40. Yokogawa N, Murakami H, Demura S, Kato S, Yoshioka K, Yamamoto M, Iseki S, Tsuchiya H. Effects of radiation on spinal dura mater and surrounding tissue in mice. *PLoS One*. 2015;10: e0133806.
41. Zibly Z, Schlaff CD, Gordon I, Munasinghe J, Camphausen KA. A novel rodent model of spinal metastasis and spinal cord compression. *BMC Neurosci*. 2012;13:137.